SOME IMPROVEMENTS TO THE FDTD ALGORITHM FOR THE ANALYSIS OF PASSIVE CIRCUITS

R. C. Tupynambá and A. S. Omar

Arbeitsbereich Hochfrequenztechnik
Technische Universität Hamburg-Harburg — Germany

Abstract

A new graded lattice mesh scheme for the FDTD is presented, in which the location of the different materials in the structure is taken into account. This makes it possible to maintain the efficiency of other graded lattice schemes without the big increasing of memory requirements they imply.

A new compensated non-matched source is also presented which uses the results of a 2D-FDTD analysis to distinguish between the incident and the reflected parts of the signal on the excitation plane. This solution is time-saving as compared to the traditional method of using a long line at the input or with the 3D analysis for the matched source.

The 2D-FDTD analysis is the same as from other authors, but at the first time with a rigorous description, without using complex numbers for real time-domain field components.

1 Introduction

Since 1966, when Yee proposed his uniform mesh [1] for the finite difference time domain (FDTD) analysis of electromagnetic problems, a lot of advances have been made in order to get the method more efficient. [2] presents a graded mesh which is able to concentrate the computational efforts in the direction of more variations. [3] presents the subgridding method which can consider in details the regions where the field is more concentrated. [4] shows a graded scheme, where this can be made more efficiently. The scheme we introduce here is an improvement of these ones, where we take into account the geometry of the different materials in the structure to proceed the division of the space. We make a first division of the space according to the material interfaces, so that each region is homogeneous. Then we can divide each region uniformly, like in [2]. This makes the method more efficient than in [4], because the corrections to achieve second order accuracy are made only at the board of the regions, and we have lower memory requirements, because the coefficients for the up-date equations in each region are the same in all cells.

Secondly, we present a new strategy to separate incident and reflected pulses at the input of the structure under analysis. The traditional solution for this problem, such as in [5], is based on taking enough long line at the input, so that the reflected pulse will only be present when the incident pulse has already vanished. Another solution is the matched source [6], where one has to calculate the incident impulse in a separate line and store the time domain data for later use. The solution we present here consists on calculating the characteristics of the input line through a two dimensional FDTD which is very faster as the 3D calculation. This can substitute the above mentioned methods with very lower memory and CPU time requirements.

In the 2D-FDTD algorithm presented in [4] and [7], the authors have used the complex propagation equation for the frequency domain in the time domain, coming to a false equation which could still lead to a correct algorithm through some manipulations. Here we present a rigorous description of the method to prove that the algorithm was in fact right.

2 Graded lattice

The first division of the structure we make is according to the interfaces between the different materials. Fig. 1 shows the division of a two dimensional cut of a coplanar waveguide as an example.

After this division has been made, the type of the six walls of each region should be assigned, whether electric or magnetic wall, absorbing boundary, part of a structure port, or neighbour of an adjacent region. Each region will be then divided uniformly along each direction in cells and the field components will be calculated normally as an independent structure. The only different step is the calculation of the electric field tangential to the interface between two neighbouring regions.

In order to explain this calculation we will show a 2D cut of a mesh in the neighbourhood of an interface normal to the x-direction, and calculate E_z at this interface (Fig. 2). In the general case, $\partial H_y/\partial x$ will not be continuous at this interface, so that this derivative cannot be interpolated like in [4]. What we do is the extrapolation of H_y at the side where the cells are coarser to the point B, so that A and B are equidistant from the interface. This extrapolation is made using a second order trace of the field at the points C, D and E, to maintain the second order accuracy, like in equation

CH3577-4/95/0000-1657$01.00 © 1995 IEEE

1995 IEEE MTT-S Digest

(1). This side of the interface is chosen for this extrapolation to permit the ratio between the cell lenghts to be much greater than five.

$$\begin{aligned} H_y(B) &= H_y(C)\frac{(3\Delta x - \Delta x')(5\Delta x - \Delta x')}{8\Delta x^2} \\ &+ H_y(D)\left(1 - (\frac{3\Delta x - \Delta x'}{2\Delta x})^2\right) \\ &+ H_y(E)\frac{(3\Delta x - \Delta x')(\Delta x - \Delta x')}{8\Delta x^2} \end{aligned} \quad (1)$$

With H_y defined at the points A and B, and H_x at the conventional points of the mesh F and G, it is possible to derive the up-date equation for E_z (2) as described in [5].

$$\begin{aligned} e_z^{n+1} &= \frac{\epsilon_{rz} - \frac{\Delta t \sigma_z}{2\epsilon_o}}{\epsilon_{rz} + \frac{\Delta t \sigma_z}{2\epsilon_o}} e_z + \frac{(c\Delta t)^2}{\epsilon_{rz} + \frac{\Delta t \sigma_z}{2\epsilon_o}} \\ &\times \left(\frac{b_y(B) - b_y(A)}{(\Delta x)^2} - \frac{b_x(F) - b_x(G)}{(\Delta y)^2}\right) \end{aligned} \quad (2)$$

In the above equation Δx is the step in the coarser side of the interface, ϵ_{rz} and σ_z are the arithmetic averages of their values in the two media, and e_z, b_x and b_y represent the variable transformations shown in (3) and (4), to get the up-date equation for the magnetic field without any multiplication.

$$\begin{aligned} e_x &= \Delta x E_x \\ e_y &= \Delta y E_y \\ e_z &= \Delta z E_z \end{aligned} \quad (3)$$

$$\begin{aligned} b_x &= \frac{\mu}{\Delta t}\Delta y \Delta z H_x^{n+\frac{1}{2}} \\ b_y &= \frac{\mu}{\Delta t}\Delta x \Delta z H_y^{n+\frac{1}{2}} \\ b_z &= \frac{\mu}{\Delta t}\Delta x \Delta y H_z^{n+\frac{1}{2}} \end{aligned} \quad (4)$$

3 Compensated source

Three problems related to the input line can be solved simultaneously by using the two-dimensional FDTD. These are field distribution, matched boundary and separation between reflected and incident signals.

First of all, it is advantageous to assume the field distribution of the exciting pulse so near as possible as it is in reality in order not to take much time to acchieve this distribution during the simulation. The 2D-FDTD can provide this distribution quite fast.

Furthermore, it is important that the reflected signal at the input can be absorbed after the emission of the impulse. The 2D-FDTD can provide accurately the phase velocity of the wave propagation in the input line which can be used with good precision even with the simple Mur's first order absorbing boundary condition [8].

A more important point is to shorten the long input line necessary for the separation of incident and reflected pulses. This is possible if we make use of a well defined characteristic impedance Z_o to be calculated by the 2D-FDTD in conjunction with (5).

$$\begin{aligned} a &= \frac{V + Z_o I}{\sqrt{Z_o}} \\ b &= \frac{V - Z_o I}{\sqrt{Z_o}} \end{aligned} \quad (5)$$

4 2D-FDTD

In frequency domain, the axial depedence of the field components is given by (6). Making use of the conjugate expression with the negative frequencies it is easy to derive this dependence in the time domain as given by (7), where '^' denotates the Hilbert-transform.

$$\psi(z) = \psi(0)e^{-j\beta z} \quad (6)$$

$$\psi(z) = \Re\{e^{-j\beta z}[\psi(0) - j\hat{\psi}(0)]\} \quad (7)$$

The derivatives of each component and of each Hilbert-transform can then be calculated according to (8).

$$\begin{aligned} \frac{\partial \psi}{\partial z} &= -\beta \hat{\psi} \\ \frac{\partial \hat{\psi}}{\partial z} &= \beta \psi \end{aligned} \quad (8)$$

Substituting this derivatives in Maxwell equations and making use of the variable transformations given by (9) and (10), one can find the up-date equations (11) and (12), once more without any multiplication for the magnetic field calculation.

$$\begin{aligned} b_x &= \frac{\mu \Delta y}{\beta \Delta t}\hat{H}_x^{n+\frac{1}{2}} \\ b_y &= \frac{\mu \Delta x}{\beta \Delta t}\hat{H}_y^{n+\frac{1}{2}} \\ b_z &= \frac{\mu \Delta x \Delta y}{\Delta t}H_z^{n+\frac{1}{2}} \end{aligned} \quad (9)$$

$$\begin{aligned} e_x &= \Delta x E_x \\ e_y &= \Delta y E_y \\ e_z &= \frac{1}{\beta}\hat{E}_z \end{aligned} \quad (10)$$

$$b_x = b_x^{n-1} - (e_z - e_z^{j-1} - e_y) \quad (11)$$

$$e_x^{n+1} = \frac{1 - \frac{\sigma \Delta t}{2\epsilon}}{1 + \frac{\sigma \Delta t}{2\epsilon}} e_x + \frac{(c\Delta t)^2}{\epsilon_r (1 + \frac{\sigma \Delta t}{2\epsilon})} \times \left(\frac{b_z^{j+1} - b_z}{(\Delta y)^2} + \beta^2 b_y \right) \quad (12)$$

With these up-date equations for some values of β and an initial field distribution, one can obtain the desired results very faster and with the same precision as in a 3D analysis. The only requirement for the initial field distribution is that it must excite the desired mode predominantly. An electric field equal unity along the segment where the voltage is calculated was enough in all of the several cases we have analysed, such as microstrip, CPW, finline or rectangular waveguide.

5 Numerical results

To validate our algorithm, we have analysed the same structure as in [4], a microstrip low-pass filter shown in Fig. 3. Fig. 4 shows the return loss of this filter calculated in that paper using a grading of 1:2 in the mesh and our calculation using the variable grading according to the location of the materials. Our calculation utilized 56 × 24 × 16 cells and required a CPU-time of 18 minutes on a CONVEX C3840. The two calculations agree to a very good extent.

6 Conclusions

A new method of dividing the structure for the FDTD analysis has been presented which considers the interfaces between materials in order to decrease the memory requirements and acchieve the efficiency of other graded lattice methods. A new method for obtaining a compensated source has been presented which reduces the computation time in comparison to previous methods. This method is based on making use of a 2D-FDTD which has been described rigorously. Computed results have shown a good agreement with calculations of other methods.

7 Aknowledgments

This work was partly supported by Deutscher Akademischer Austauschdienst — DAAD, Germany and by Conselho Nacional de Desenvolvimento Científico e Tecnológico — CNPq, Brasília, Brazil.

References

[1] Yee, K. S. — "Numerical solution of initial boundary value problems involving Maxwell's equations in isotropic media" — IEEE Trans. Antennas Propagat., vol. AP-14, pp. 302 - 7, May 1966.

[2] Choi, D. H. and Hoefer, W. F. R. — "A graded mesh FDTD algorithm for eigenvalue problems" — 17th European Microwave Conference Digest, pp. 413 - 7, 1987.

[3] Zivanovic, S. S., Yee, K. S. and Mei, K. K. — "A subgridding method for the FDTD method to solve Maxwell's equations" — IEEE Trans. Microwave Theory Tech., vol. MTT-39, pp. 471 - 9, March 1991.

[4] Xiao, S. and Vahldieck, R. — "An improved 2D-FDTD algorithm for hybrid mode analysis of quasi-planar transmission lines" — 1993 IEEE MTT-Symposium Digest, pp. 421 - 4, 1993.

[5] Liang, G., Liu, Y. and Mei, K. K. — "Full-wave analysis of coplanar waveguide and slotline using the time-domain finite-difference method" — IEEE Trans. Microwave Theory Tech., vol. MTT-37, pp. 1949 - 57, December 1989.

[6] Rittweger, M. and Wolff, I. — "Analysis of complex passive (M)MIC-components using the finite difference time-domain approach" — 1990 IEEE MTT-Symposium Digest, pp. 1147 - 50, 1990.

[7] Brankovic, V. J., Krupezevic, D. V. and Arndt, F. — "An efficient two-dimensional graded mesh finite-difference time-domain algorithm for shielded or open waveguide structures" — IEEE Trans. Microwave Theory Tech., vol. MTT-40, pp. 2272 - 7, December 1992.

[8] Mur, G. — "Absorbing boundary conditions for finite-difference approximation of the time-domain electromagnetic field equations" — IEEE Trans. Electromagn. Compat., vol. EMC-23, pp. 1073 - 7, November 1981.

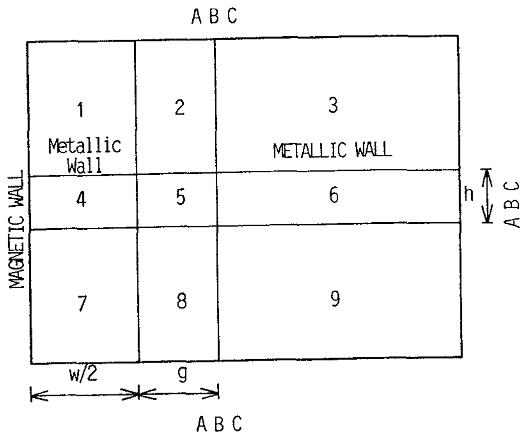

Figure 1: CPW cut divided in nine regions

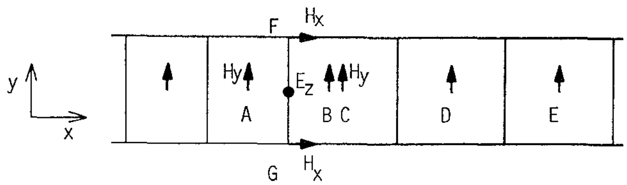

Figure 2: Interface between two regions

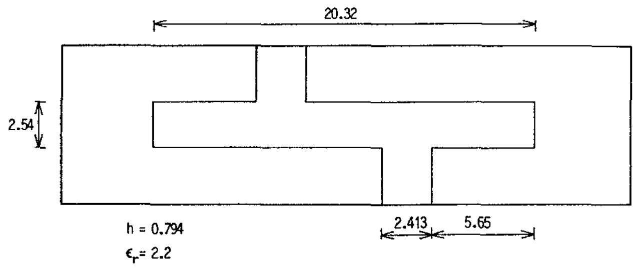

Figure 3: Microstrip low-pass filter

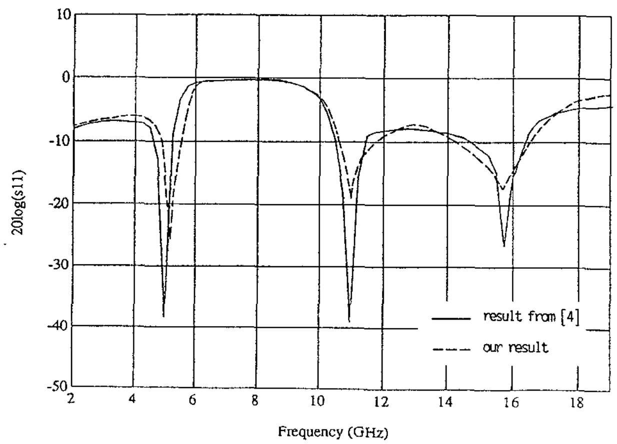

Figure 4: Filter return loss